Letters

ENSO-Forced Variability of the Pacific Decadal Oscillation

MATTHEW NEWMAN, GILBERT P. COMPO, AND MICHAEL A. ALEXANDER

NOAA–CIRES Climate Diagnostics Center, University of Colorado, Boulder, Colorado

5 March 2003 and 12 June 2003

ABSTRACT

Variability of the Pacific decadal oscillation (PDO), on both interannual and decadal timescales, is well modeled as the sum of direct forcing by El Niño–Southern Oscillation (ENSO), the ''reemergence'' of North Pacific sea surface temperature anomalies in subsequent winters, and white noise atmospheric forcing. This simple model may be taken as a null hypothesis for the PDO, and may also be relevant for other climate integrators that have been previously related to the PDO.

1. Introduction

Studies of sea surface temperatures (SST) in the North Pacific have focused on the Pacific decadal oscillation (PDO) as the leading mode of variability, particularly on decadal timescales (Mantua et al. 1997). There is considerable uncertainty, however, about whether the PDO is truly independent of the leading mode of tropical variability, El Niño–Southern Oscillation (ENSO; Zhang et al. 1997; Evans et al. 2001). On the one hand, simultaneous correlations of the November–March mean PDO index with various indices of ENSO are low (Mantua et al. 1997). In addition, the spatial patterns of SST variability in the Pacific on interannual and decadal timescales are different; interannual variability of SST exhibits the pronounced ENSO maximum in the tropical east Pacific and a weaker center of opposite sign in the North Pacific, while on decadal timescales the relative strength of these centers is reversed so that the amplitude of the tropical maximum is about 75% that of the North Pacific center (Zhang et al. 1997).

On the other hand, weak *simultaneous* correlation between ENSO and the PDO may be misleading. Anomalous tropical convection induced by ENSO influences global atmospheric circulation and hence alters surface fluxes over the North Pacific, forcing SST anomalies that peak a few months after the ENSO maximum in tropical east Pacific SSTs (Trenberth and Hurrell 1994; Alexander et al. 2002). This ''atmospheric bridge'' explains as much as half of the variance of January–March seasonal mean anomalies of SST in the central North Pacific (Alexander et al. 2002). Furthermore, North Pacific SSTs have a multiyear memory during the cold season. Deep oceanic mixed layer temperature anomalies from one winter become decoupled from the surface during summer and then ''reemerge'' through entrainment into the mixed layer as it deepens the following winter (Alexander et al. 1999). Thus, over the course of years, at least during winter and spring, the North Pacific integrates the effects of ENSO.

The prevailing *null hypothesis* of midlatitude SST variability posits that the ocean integrates forcing by unpredictable and unrelated weather, approximated as white noise, resulting in ''reddened'' noise with increased power at low frequencies and decreased power at high frequencies (e.g., Frankignoul and Hasselmann 1977). In this paper, we propose an expanded null hypothesis for the PDO: variability in North Pacific SST on seasonal to decadal timescales results not only from red noise but also from reddening of the ENSO signal.

2. Data and results

The analysis described in this paper is based on simple indices of SST and atmospheric variability for the years 1900–2001. SSTs are from the Hadley Sea Ice and Sea Surface Temperature analysis (Rayner et al. 2003) for the years 1900–99 and from the National Oceanic and Atmospheric Administration (NOAA) reconstructed SST (Smith et al. 1996) dataset for 2000–01. Both datasets are on a $1^\circ \times 1^\circ$ grid. Monthly mean anomalies were determined by removing the 1950–2001 climatological monthly means; empirical orthogonal functions (EOFs) are determined for this period. Very

Corresponding author address: Matthew Newman, NOAA–CIRES Climate Diagnostics Center, Mail Code R/CDC, 325 Broadway, Boulder, CO 80303-3328.
E-mail: matt.newman@noaa.gov

similar results were obtained by instead using the NOAA dataset for the 1950–2001 period, and/or by computing the EOFs separately for each month.

The PDO index is determined by projecting SST on the leading EOF of monthly SST in the Pacific north of 20°N (Mantua et al. 1997). The ENSO index is determined by projecting SST on the leading EOF of monthly SST in the region 20°N–20°S, 120°E–60°W; similar results are obtained with other ENSO indices. Atmospheric variability is represented by the North Pacific index (NPI; Trenberth and Hurrell 1994), an average of sea level pressure (SLP) in the region 30°–65°N, 160°E–140°W. The NPI measures the strength of the Aleutian low during the Northern Hemisphere cold season, and it encompasses the area of maximum SLP variance in the North Pacific for all months. All indices are departures from the annual cycle, subjected to a three-month running mean, detrended over the 102-yr record, and normalized to have unit variance. Prior to 1950, the general paucity of data may make month-to-month variation of the SST indices unreliable. Thus, the seasonal cycle of correlation is only calculated for the 1950–2001 period, while all other analyses, which focus on timescales of 1 yr and greater, use the entire record. Detrending the 1950–2001 period (not shown) somewhat reduces the autocorrelation of the PDO and its power for periods greater than 20 yr but does not notably impact the ENSO–PDO relationship (see also Livezey and Smith 1999).

Pronounced seasonality of the PDO is seen in its annual cycle of lag autocorrelation (Fig. 1a), with a maximum in late winter/early spring (indicated by the black diagonal dashed lines) and a minimum in summer and fall. The correlation between March of year 0 and March of year 2 (i.e., March + lag 24) is 0.39, whereas between July of year 0 and July of year 2 it is 0.19; the correlation from one November to any November is near zero. Thus, for lags greater than a year the PDO persists from winter to winter but does not persist (at least at the surface) through the summer in between, consistent with reemergence (e.g., Deser et al. 2003).

The PDO is often associated with the NPI, but the persistence of North Pacific SST anomalies is only weakly reflected in the atmosphere. The NPI has year-to-year correlation (Fig. 1b) that is near zero ($r = 0.05$) in winter and reaches a maximum in spring of only 0.25, which is just over the 90% significance level. Moreover, during winter the NPI leads the PDO not only on monthly timescales, but also on annual timescales (Fig. 1c); in January, the amplitude of the NPI–PDO correlation for a 1-yr interval is 0.32 when the atmosphere leads the ocean but is 0.13 when the ocean leads the atmosphere.

ENSO also leads the PDO index by a few months throughout the year (Fig. 1d), most notably in winter and summer. Simultaneous correlation is lowest in November–March, consistent with Mantua et al. (1997). The lag of maximum correlation ranges from two months in summer ($r \sim 0.7$) to as much as five months by late winter ($r \sim 0.6$). During winter and spring, ENSO leads the PDO for well over a year, consistent with reemergence of prior ENSO-forced PDO anomalies. Summer PDO appears to lead ENSO the following winter, but this could be an artifact of the strong persistence of ENSO from summer to winter ($r = 0.8$), combined with ENSO forcing of the PDO in both summer and winter. Note also that for intervals less than 1

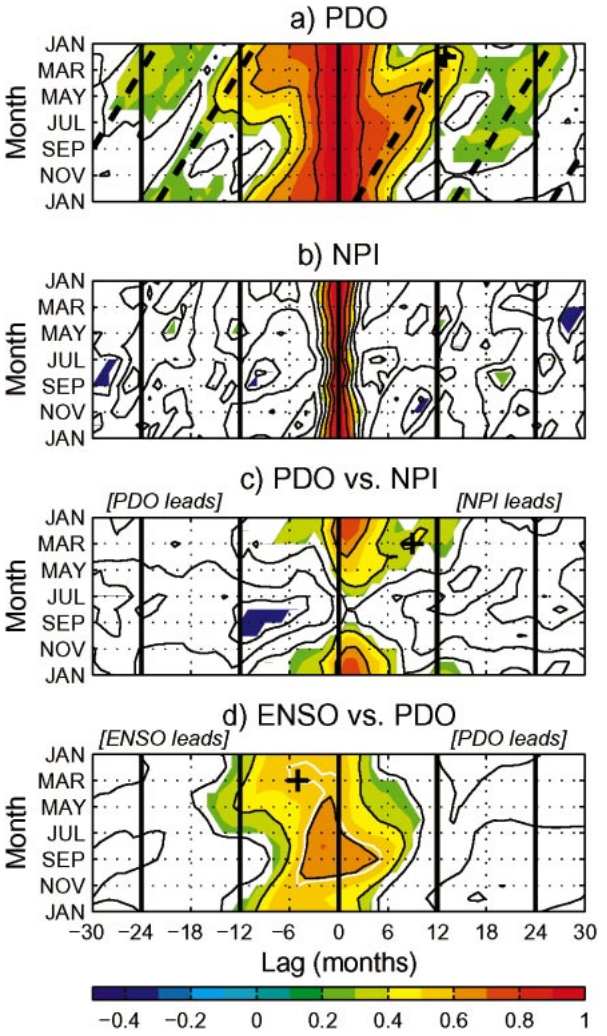

FIG. 1. (a) Annual cycle of PDO autocorrelation, plotted as a function of month. Heavy dashed lines indicate correlation with Mar PDO; e.g., the cross represents correlation of the PDO in Feb of year 0 and Mar of year 1 (i.e., lag +13). (b) Same as (a) but for the NPI. (c) Annual cycle of cross correlation between the PDO and the NPI. The NPI leads the PDO for positive lags; the PDO leads the NPI for negative lags. The month ordinate refers to the NPI; e.g., the cross represents correlation between Mar NPI and Dec (lag +9) PDO. (d) Annual cycle of cross correlation between ENSO and the PDO. The PDO leads ENSO for positive lags; ENSO leads the PDO for negative lags. The month ordinate refers to the PDO; e.g., the cross represents correlation between Mar PDO and Oct (lag −5) ENSO. The thin white line is the 0.58 contour. Correlations are for the period 1950–2001, and contour (fill) interval is 0.2 (0.1). Only values that are at least 90% significant are shaded.

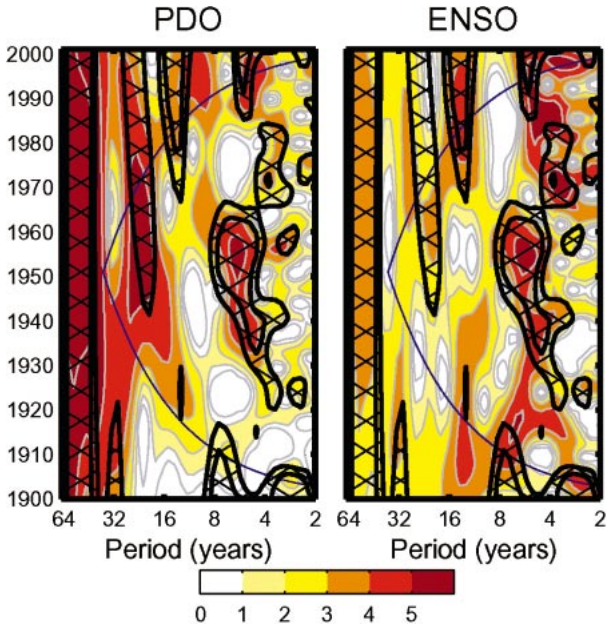

FIG. 2. Wavelet power spectrum of (left) PDO and (right) ENSO indices. Shading corresponds to $\log_2$(power); contours for values less than zero are omitted for clarity. The blue line indicates the cone of influence. Wavelet squared coherence exceeding 0.75 is indicated with the black contours (0.75 and 0.9) and hatching. Within the cone of influence, coherence of 0.76 (0.81) is 90% (95%) significant, based on a Monte Carlo simulation between 1000 sets (two each) of white noise time series.

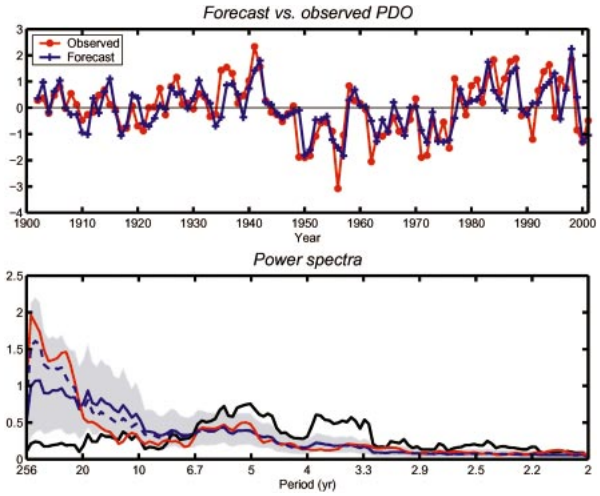

FIG. 3. Null hypothesis model of annual mean PDO. (top) Time series of ''forecast'' and observed PDO. (bottom) Power spectra of observed PDO (red), ENSO (black), and ensemble mean ''model'' PDO (blue) indices. The 95% confidence interval, shown by gray shading, is determined from the two-sided distribution of 1000 100-yr samples of the ''model'' PDO. The dashed blue line indicates the mean of the 20% (200 100-yr samples) of the ''model'' PDO spectra with minimum std dev from the observed PDO power spectrum.

yr the lag autocorrelation of the PDO is low when the lag autocorrelation of ENSO (not shown) is also low, through the so-called spring persistence barrier (Torrence and Webster 1998).

The relationship between ENSO and the PDO extends to longer timescales. Wavelet analysis (Torrence and Compo 1998) shows that variations of spectral power as a function of both time and period are similar for each index (Fig. 2). Significantly, the two power spectra are almost always highly coherent (Torrence and Webster 1999) when the PDO has high power. Coherence (hatching) does not imply similar amplitude, however. The PDO is much redder than ENSO, so at short (long) periods the coherent ENSO signal tends to be stronger (weaker) than the PDO. Overall, about (54%, 32%, 30%) of the variance of (PDO, ENSO, NPI) seasonal means (respectively) is at periods of 10 yr and greater.

Using the wavelet analysis as a filter, we find a high (0.71) correlation between the PDO and ENSO in the 4–9-yr band. Retaining only periods longer than 10 yr results in a correlation of 0.61; as this cutoff is increased the correlation between the two indices also increases, reaching 0.98 when retaining periods greater than 40 yr.

The wavelet results suggest that the North Pacific acts to redden not only atmospheric noise, as in the standard null hypothesis, but also the ENSO signal, an effect that should be included in the ''background'' power spectrum before purely extratropical modes of decadal variability can be identified. Despite strong seasonality of the PDO–ENSO relationship, both Fig. 1 and mixed layer dynamics (Deser et al. 2003) suggest that a *very simple* model of this reddening behavior can be written for annual (July–June) averaged anomalies, as

$$P_n = \alpha P_{n-1} + \beta E_n + \eta_n, \qquad (1)$$

where P is the model PDO index, E is the (observed) ENSO index, n is time (in years), and η is uncorrelated (and unpredictable) noise. Recall $\langle P_n^2 \rangle = \langle E_n^2 \rangle = 1$, where brackets represent a time or ensemble mean. Parameters $\alpha = 0.58$ and $\beta = 0.58$ are obtained from observations by regressing the PDO against ENSO, removing the ENSO term, and then regressing the residual against the previous year's PDO. Note that α is on the upper end of the range derived from a mixed layer model of North Pacific reemergence (Deser et al. 2003).

That (1) is a better simple model of PDO variability than a first-order autoregressive (AR1) model can be seen by making forecasts $\hat{P}_n = \alpha P_{n-1} + \beta E_n$. The forecasts were cross validated by removing 10 yr from the data, computing α and β from the remaining data, using this α and β to make forecasts for the missing years, and so on. This produced values of α and β that varied by no more than $\pm 5\%$. (Similar skill was also obtained by splitting the data in half.) Forecast and observed PDO (shown in Fig. 3a) are correlated at 0.74. This skill is significantly better (at the 95% level) than either an AR1 model or using just βE_n to forecast the PDO, which yielded cross-validated correlation skills of 0.53 and 0.57, respectively. In addition, the rms forecast error using $\hat{P}_n$ is about 20% less than for these other models.

Using (1), 1000 realizations of 100-yr-long time series are generated. The observed PDO and ENSO spectra and the ensemble mean of the model spectra, determined using the Thomson multitaper method, are shown in Fig. 3b. The ensemble mean model PDO is much redder than ENSO, since the expected power spectrum $\langle P_T^2 \rangle$ resulting from (1) is

$$\langle P_T^2 \rangle = \frac{(\beta E_T)^2 + \langle \eta_T^2 \rangle}{1 - 2\alpha \cos(2\pi/T) + \alpha^2}, \qquad (2)$$

where E_T is the Fourier transform of E_n, η_T is the Fourier transform of η_n, and T is the period in years. For $\alpha = 0.58$, the denominator of (2) is less than 1 for $T > 5$ yr. Thus, the PDO response to ENSO forcing is amplified for decadal timescales.

The observed PDO is not only redder than ENSO, it is redder than the model ensemble mean $\langle P_T^2 \rangle$. This could represent independent extratropical decadal variability; alternatively, a two-index model certainly oversimplifies tropical–extratropical interaction. Note, however, that the observed spectrum is well within the 95% confidence interval of (1), showing that the short data record implies considerable uncertainty regarding the ''true'' underlying spectrum, particularly for periods greater than 10 yr. The reddening effect of (2) also increases the spread of this uncertainty at long periods. Moreover, many individual model spectra also have higher power than $\langle P_T^2 \rangle$ on long (>20 yr) periods and less power on intermediate (10–20 yr) periods, as is shown in an average of a large subset (20%) of model spectra (Fig. 3).

3. Conclusions

The PDO is dependent upon ENSO on *all* timescales. To first order, the PDO can be considered the reddened response to both atmospheric noise and ENSO, resulting in more decadal variability than either. This null hypothesis needs to be considered when diagnosing and modeling ''internal'' decadal variability in the North Pacific. For example, the observed spatial pattern of Pacific SST decadal variability, with relatively higher amplitude in the extratropics than in the Tropics, should be at least partly a consequence of a reddened ENSO response.

It has been suggested that decadal variability in the North Pacific may be more prominent during summer than during winter (e.g., Zhang et al. 1998). Our results suggest just the opposite: the PDO has little multiyear persistence during summer, so decadal variability of North Pacific SST is largely a winter/spring phenomenon. The confusion occurs because there is some correlation of the PDO between *consecutive* summers, but this is likely a consequence of the annual cycle of ENSO and the strong ENSO–PDO relationship that exists in both summer and winter (Fig. 1d); that is, a growing ENSO forces the PDO in summer, the subsequent mature phase of ENSO forces the PDO the following winter/spring, and this North Pacific SST anomaly then persists into the early part of the following summer.

Figure 1 also shows that correlating atmospheric variables of interest to the PDO index to determine variability possibly ''caused'' by the PDO, as well as stratifying the extratropical response to ENSO by ''high'' and ''low'' PDO events (e.g., Gershunov and Barnett 1998), may just reproduce an ENSO signal plus variations due to atmospheric noise. Again, such analyses may be particularly problematic during summer. Conversely, differentiating between the PDO and ENSO may still be of interest during spring (Alexander et al. 2002), especially during post-ENSO years.

Consistent with earlier studies, the NPI results suggest that the atmospheric component of North Pacific decadal variability is weaker than the SST component. Why, then, are pronounced PDO signals found remotely over North America in drought (Barlow et al. 2001) and in climate proxies such as tree rings (Biondi et al. 2001; D'Arrigo et al. 2001)? One possibility is that North Pacific SST is not the only variable that can be modeled in the form of (1). Other such ''climate integrators'' will correlate with the PDO simply because they too redden ENSO. For example, tree-rings and soil moisture both have anomalies with decorrelation times on the order of a few years (e.g., Fritts 1976; Huang et al. 1996), so they could integrate ENSO forcing in a manner similar to, but not necessarily forced by, the North Pacific.

Finally, this work suggests that predicting the PDO may be directly related to the skill of forecasting ENSO. Given the 2-yr decorrelation timescale of the PDO and the possibility that ENSO may not be predictable beyond about 2 yr, so-called regime shifts of the PDO will not be apparent until years after they have occurred. For example, the recent long-term positive phase of the PDO may have simply resulted from the 1977–98 period being dominated by warm events in the Tropics, and the recent apparent ''change'' in phase of the PDO is an expected outcome of the cool tropical SST in the east Pacific of the last few years. Thus, with tropical SSTs having returned to warm conditions in 2002, the PDO has likewise become positive again. In the absence of a La Niña this year, the PDO may be expected to remain positive in 2004.

Acknowledgments. Comments from J. Barsugli, I. Bladé, C. Deser, A. Miller, C. Penland, P. Sardeshmukh, C. Smith, and an anonymous reviewer are appreciated. R. Webb and M. Dettinger invited MN to give a preliminary version of this study at the 2001 PACCLIM conference. C. Winkler assisted in the preparation of Fig 2. This work was partially supported by a grant from NOAA CLIVAR/Pacific.

REFERENCES

Alexander, M. A., C. Deser, and M. S. Timlin, 1999: The re-emergence of SST anomalies in the North Pacific Ocean. *J. Climate,* **12,** 2419–2431.

——, I. Bladé, M. Newman, J. R. Lanzante, N.-C. Lau, and J. D. Scott, 2002: The atmospheric bridge: The influence of ENSO teleconnections on air–sea interaction over the global oceans. *J. Climate,* **15,** 2205–2231.

Barlow, M., S. Nigam, and E. H. Berbery, 2001: ENSO, Pacific decadal variability, and U.S. summertime precipitation, drought, and streamflow. *J. Climate,* **14,** 2105–2128.

Biondi, F., A. Gershunov, and D. R. Cayan, 2001: North Pacific decadal climate variability since 1661. *J. Climate,* **14,** 5–10.

D'Arrigo, R., R. Villalba, and G. Wiles, 2001: Tree-ring estimates of Pacific decadal climate variability. *Climate Dyn.,* **18,** 219–224.

Deser, C., M. A. Alexander, and M. S. Timlin, 2003: Understanding the persistence of sea surface temperature anomalies in midlatitudes. *J. Climate,* **16,** 57–72.

Evans, M. N., M. A. Cane, D. P. Schrag, A. Kaplan, B. K. Linsley, R. Villalba, and G. M. Wellington, 2001: Support for tropically-driven Pacific decadal variability based on paleoproxy evidence. *Geophys. Res. Lett.,* **28,** 3689–3692.

Frankignoul, C., and K. Hasselmann, 1977: Stochastic climate models. Part II: Application to sea-surface temperature anomalies and thermocline variability. *Tellus,* **29,** 284–305.

Fritts, H. C., 1976: *Tree Rings and Climate.* Academic Press, 567 pp.

Gershunov, A., and T. P. Barnett, 1998: Interdecadal modulation of ENSO teleconnections. *Bull. Amer. Meteor. Soc.,* **79,** 2715–2725.

Huang, J., H. M. Van den Dool, and K. P. Georgakakos, 1996: Analysis of model-calculated soil moisture over the United States (1931–1993) and applications to long-range temperature forecasts. *J. Climate,* **9,** 1350–1362.

Livezey, R. E., and T. M. Smith, 1999: Covariability of aspects of North American climate with global sea surface temperatures on interannual to interdecadal timescales. *J. Climate,* **12,** 289–302.

Mantua, N. J., S. R. Hare, Y. Zhang, J. M. Wallace, and R. Francis, 1997: A Pacific interdecadal climate oscillation with impacts on salmon production. *Bull. Amer. Meteor. Soc.,* **78,** 1069–1079.

Rayner, N. A., D. E. Parker, E. B. Horton, C. K. Folland, L. V. Alexander, D. P. Rowell, E. C. Kent, and A. Kaplan, 2003: Global analyses of sea surface temperature, sea ice, and night marine air temperature since the late nineteenth century. *J. Geophys. Res.,* **108,** 4407, doi:10.1029/2002JD002670.

Smith, T. M., R. W. Reynolds, R. E. Livezey, and D. C. Stokes, 1996: Reconstruction of historical sea surface temperatures using empirical orthogonal functions. *J. Climate,* **9,** 1403–1420.

Torrence, C., and G. P. Compo, 1998: A practical guide to wavelet analysis. *Bull. Amer. Meteor. Soc.,* **79,** 61–78.

——, and P. J. Webster, 1998: The annual cycle of persistence in the El Niño–Southern Oscillation. *Quart. J. Roy. Meteor. Soc.,* **124,** 1985–2004.

——, and ——, 1999: Interdecadal changes in the ENSO-monsoon system. *J. Climate,* **12,** 2679–2690.

Trenberth, K., and J. Hurrell, 1994: Decadal atmosphere–ocean variations in the Pacific. *Climate Dyn.,* **9,** 303–319.

Zhang, Y., J. M. Wallace, and D. S. Battisti, 1997: ENSO-like interdecadal variability. *J. Climate,* **10,** 1004–1020.

——, J. R. Norris, and J. M. Wallace, 1998: Seasonality of large-scale atmosphere–ocean interaction over the North Pacific. *J. Climate,* **11,** 2473–2481.